

Cover Page



Universiteit Leiden



The handle <http://hdl.handle.net/1887/20094> holds various files of this Leiden University dissertation.

Author: Melis, Joost

Title: Nucleotide excision repair in aging and cancer

Date: 2012-11-06



Chapter 4

Chapter 4

Mutational and transcriptional responses upon oxidative damage exposure in $Xpc^{-/-}$ mice

Melis JPM, Kuiper RV, Pennings JLA, Zwart E, Robinson J, van Oostrom CTM, Luijten M, van Steeg H.

Mutational and transcriptional responses upon oxidative damage exposure in $Xpc^{-/-}$ mice

Revisions, Antioxidants & Redox Signaling (Special Issue December 2012)

*"Yes, there are two paths you can go by, but in the long run,
There's still time to change the road you're on"*

Stairway To Heaven – Led Zeppelin, 1971

Abstract

The Nucleotide Excision Repair (NER) pathway is one of the main and most versatile mechanisms preventing DNA damage accumulation and subsequent cancer development. Previously we demonstrated that NER-deficient mouse models *Xpa*^{-/-} and *Xpc*^{-/-} are both cancer prone, but exhibit a divergent tumor spectrum and incidence. Here, we report, *in vitro* and for the first time *in vivo*, that *Xpc*^{-/-} mice are more sensitive to exogenously induced oxidative DNA damage.

Xpc^{-/-} mouse embryonic fibroblasts exposed to normoxic and atmospheric oxygen pressures were more sensitive to atmospheric oxygen levels and showed a significantly increased mutational load, contrary to wild type and *Xpa*^{-/-} cells. Additionally, comprehensive *in vivo* studies in wild type, *Xpa*^{-/-} and *Xpc*^{-/-} mice with the pro-oxidants DEHP and paraquat increased oxidative stress levels in liver of all genotypes, indicated by amongst others the level of lipofuscin accumulation. After long-term pro-oxidant exposures *Xpc*^{-/-} mice, but not *Xpa*^{-/-} and wild type mice, revealed significantly elevated mutational levels in liver. Transcriptomic analyses provided insight into this divergent response between *Xpa*^{-/-} and *Xpc*^{-/-} mice. Gene expression profiles overall were similar between all genotypes. However, *Xpc*^{-/-} mice, compared to wild type and *Xpa*^{-/-}, showed a lower transcriptional glutathione metabolism response, corroborating previous *in vitro* results by others. Our studies reveal that long-term *in vivo* XPC deficiency contributes to an increased oxidative DNA damage accumulation and subsequent mutational load. These findings further support our view that the XPC protein has a cancer prevention function outside of NER, which is involved in the prevention of oxidative DNA damage.

Introduction

The excessive amount of genomic assaults in cells, either by endogenous or exogenous factors, results into billions of lesions in the human body per day [1]. These lesions can result into persistent DNA damage if left unattended, and subsequently can cause cell death, cancer and accelerated aging due to loss of homeostasis [2,3].

In the defense against induced DNA damage DNA repair mechanisms are vital. Several DNA repair pathways cooperate to minimize the detrimental impact of the genomic insults. Damaged or incorrect bases can be corrected by amongst others base excision repair (BER) and nucleotide excision repair (NER). BER is mainly responsible for the removal of oxidative DNA damage [4,5], while the NER pathway is known to be accountable for removing bulky and helix-distorting lesions in the DNA [3]. However, overlap between the latter two pathways has been proposed [6-11].

In NER, over 30 proteins are involved in the complete removal and repair of the DNA lesions [3]. Two pivotal proteins in this cascade are XPA and XPC, which belong to the family of XP proteins linked to the severe autosomal recessive disorder Xeroderma pigmentosum (XP). XP in humans is marked by a 1,000-fold increased risk for sunlight-induced skin cancer [1]. Fewer than 40% of individuals with the disease, of which XP-A and XP-C patients are the most common worldwide, survive beyond age 20 years [1,12-14].

The NER pathway can be divided in two sub-pathways: global genome NER (GG-NER), which covers repair genome-wide, and transcription coupled NER (TC-NER), which is responsible for repair of the transcribed strand of active genes [1,15,16]. XP-C patients are only defective in the GG-NER pathway, while XP-A patients are hampered in both GG-NER and TC-NER sub-pathways [3].

In mice, similar characteristics to the human disorders can be mimicked by knocking out one of these XP genes. In a previous study we presented the spontaneous phenotypes of the *Xpa*- and *Xpc*-deficient knock-out mouse models in a congenic C57BL/6J background [17]. We established that *Xpa*^{-/-} and *Xpc*^{-/-} mice (hereafter referred to as *Xpa* and *Xpc*, respectively) are both cancer prone and, although being part of the same DNA repair pathway, show a divergent tumor phenotype. Compared to wild type C57BL/6J mice, both mouse models showed an increase in hepatocellular tumors (10% in *Xpa*, 13% in *Xpc*), but strikingly *Xpc* also exhibited an even higher incidence of lung tumors (16%). Mutant frequency analyses demonstrated that the tumor phenotype could be correlated to the mutational load, which accumulated over time in these mouse models. A significant increase in *LacZ* mutant levels in liver and lung was visible for *Xpc* mice, while *Xpa* only showed a significant increase in liver. These findings pointed towards an increased sensitivity of *Xpc* mice to oxygen exposure and a putative role of XPC in a process, besides NER, preventing or removing oxidative DNA damage.

In the present study, we examined the hypothesis whether *Xpc*-deficient cells and mice are more sensitive to exogenous oxidant exposure than *Xpa* and wild type cells and mice, plus set out to unravel part of the underlying differences by gene expression profiling.

Material & Methods

Cell culture

Primary mouse embryonic fibroblasts (MEFs) were isolated from E13.5 day embryos, all in C57BL/6J background, and genotyped and cultured as described previously [49;50]. MEFs were cultured for 3 days per passage at 3% or 20% O₂. The first passage for all groups was performed at 3% O₂, subsequently they were split to either 3% or 20% O₂ for two more passages. A minimum of three different embryos, all from different mothers, was used per genotype.

LacZ mutant frequency analyses

From frozen liver, lung or mouse embryonic fibroblasts, DNA was extracted and analyzed for mutant frequency as described previously [17]. Briefly, between 10 and 20 µg of genomic DNA were digested with HindIII for 1 h in the presence of magnetic beads recoated with *LacI-LacZ* fusion protein. Plasmid DNA was subsequently eluted from the beads and circularized with T4 DNA ligase. Next, ethanol-precipitated plasmids were used to transform *E. coli* C (*DLacZ*, *galE*-) cells. Dilutions of the transformed cells were plated on the titer plate (with X-gal) and the remainder on the selective plate (with p-gal). The plates were incubated for 15 h at 37°C. Mutant frequencies were determined as the number of colonies on the selective plates versus the number of colonies on the titer plate (times the dilution factor). Two-way ANOVA analyses and post-hoc t-tests to compare mutant frequencies between all groups were performed, and were considered significant if $p < 0.05$.

Mice

The generation and characterization of *Xpa* and *Xpc* mice has been described before [51;52]. The heterozygous mutant mouse strains, as well as C57BL/6J controls, were crossed with pUR288-*LacZ* C57BL/6J transgenic mice line 30, homozygous for *LacZ* integration on chromosome 11 [49]. Mice were genotyped by a standard PCR reaction using DNA isolated from tail tips. Primers to amplify the wild type and targeted *Xpa* and *Xpc* allele, as well as primer sequences for *LacZ* determination have been described previously [49;50]. The experimental setup of the studies was examined and agreed upon by the institute's Ethical Committee on Experimental Animals, according to national legislation. The health state of the mice was checked daily. During exposure, the animals were weighed weekly for the first eight weeks of exposure and biweekly for the remainder of the exposure study to monitor health conditions of the animals. Food uptake was measured for the first 5 weeks.

During the entire experiment, animals were kept in the same stringently controlled environment, fed *ad libitum* and kept under a normal day/night rhythm. Animals were removed from the study when found dead or moribund. Autopsy was performed on animals of all cohorts; tissues were stored for further histopathological analysis. In addition, a selective set of different tissues were snap frozen in liquid N₂ for *LacZ* mutant frequency analysis and gene expression profiling.

In vivo experimental design

Ten-week-old wild type (C57BL/6J), *Xpa* and *Xpc* mice were marked, genotyped and randomized in cohorts, in which the mice were sacrificed 39 weeks after start of the exposure. All genotypes were exposed to either control feed or the compounds di(2-ethylhexyl) phthalate (DEHP (CAS 117-81-7), 6,000 ppm, female mice) or methyl viologen (paraquat (CAS 1910-42-5), 100 ppm, male mice). All groups consisted of 20 animals.

The concentrations of DEHP (6,000 ppm) and paraquat (100 ppm) were used, and were chosen based on results of 2 year bioassay carcinogenicity testing in rodents [^{18;30}].

Histopathology

Tissue samples (amongst others liver, kidney, lung and tissues having gross lesions) of each animal were preserved in a neutral aqueous phosphate-buffered 4% solution of formaldehyde. Tissues required for microscopic examination were processed, embedded in paraffin wax, sectioned at 4µm and stained with haematoxylin and eosin. Detailed microscopic examination was performed on liver, lung and kidney of all mice and on all gross lesions suspected of being tumors or representing major pathological conditions. Non-neoplastic findings were either scored using 1) an ordinal scale (1-5) and averaged per group for comparisons or 2) based on incidence.

Unstained slides were mounted with Cytoseal-XYL (Richard-Allan Scientific, Thermo Fisher Scientific, MI, USA) and viewed under UV light for semiquantitative assessment of lipofuscin deposition.

Micro-array analysis

Total RNA was isolated with the Minikit (Qiagen) using the QIAcube (Qiagen) according to manufacturer's protocol. RNA quality was tested using automated gel electrophoresis (Bioanalyzer 2100; Agilent Technologies, Amstelveen, the Netherlands). All RNA samples passed RNA integrity number QC (>7.0). RNA samples (wild-type, *Xpa* and *Xpc* : n=6 per genotype) were amplified, labeled and hybridized to Nimblegen 12x135k *Mus musculus* microarrays as described in detail in Pennings et al. 2011 [⁵³].

Data analysis

Gene expression differences between experimental groups were compared with ANOVA. Obtained p-values were corrected for multiple testing by calculating the False Discovery Rate (FDR). Probes with a FDR<0.05 were considered significant. When multiple probes corresponding to the same gene were significant, their data were averaged to remove redundancy in further analysis.

Gene expression differences were visualized using GeneMaths XT (Applied Maths, St-Martens-Latem, Belgium). Regulated genes were analyzed for functional overrepresentation of GeneGo pathway maps and GO processes using MetaCore (www.GeneGO.com). Pathway map overrepresentation was considered significant if $p < 0.05$. Pathway- or gene set-level effects were specific for *Xpc* if it was either significant in *Xpc* and not in both WT and *Xpa*, or vice versa. Complete raw and normalized microarray

data and their MIAME compliant metadata have been deposited at GEO (www.ncbi.nlm.nih.gov/geo) under accession number GSE28296.

Results

Increased mutational load in Xpc MEFs upon atmospheric oxygen exposure

In our previous study we have shown that *Xpc*-deficient mice are more prone to lung cancer than *Xpa* and wild type mice. Additionally, mouse embryonic fibroblasts (MEFs) of *Xpc* mice are more sensitive in terms of survival to atmospheric oxygen levels than *Xpa* and wild type MEFs [17]. In the present study, we first verified if the decreased survival observed at atmospheric oxygen conditions in *Xpc* MEFs could be correlated to the amount of oxidative DNA damage that has been fixed as mutations. We therefore cultured wild type, *Xpa* and *Xpc* MEFs at either normoxic (3%) or atmospheric (20%) oxygen levels under the same conditions as in our previous study [17]. *LacZ* mutant frequency analyses revealed that in MEFs cultured at 3% oxygen pressure, the mutant frequency in both *Xpa* and *Xpc* cells was already slightly, but not significantly, increased compared to wild type cells (Figure 1). However at 20% oxygen pressure, *LacZ* mutant frequencies were only increased in *Xpc* MEFs compared to their normoxic treated controls ($p < 0.01$). The increased oxidative DNA damage in these cells demonstrated an inverse correlation with the previously found decreased survival response in *Xpc* cells [17].

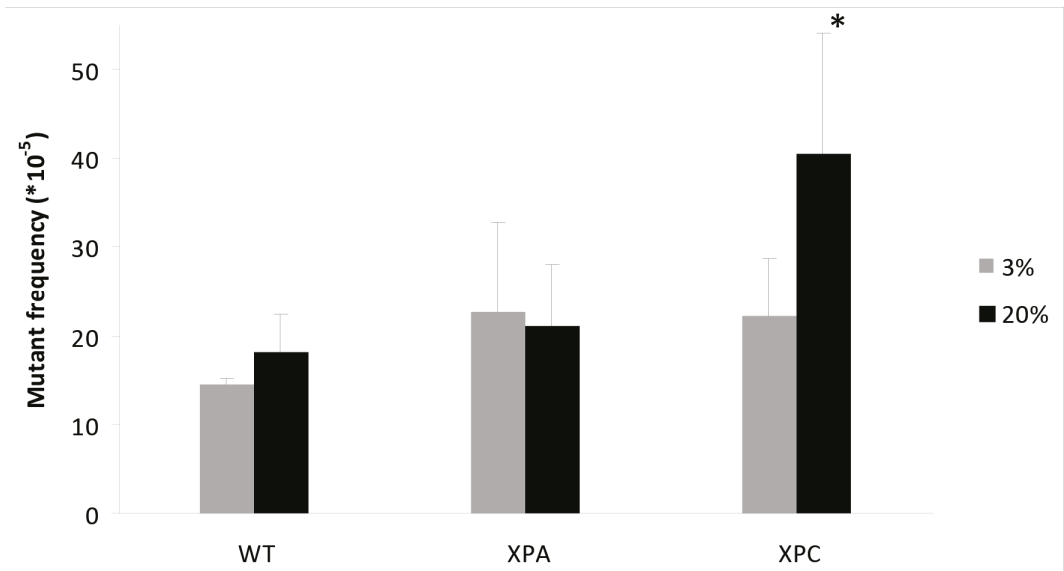


Figure 1. *LacZ* mutant frequencies in MEFs cultured at normoxic (3% O₂) or atmospheric (20% O₂) conditions. MEFs were cultured at 3% O₂ pressure the first passage and for two subsequent passages at either 3% or 20% oxygen pressure. Error bars indicated SD. * $p < 0.01$ 20% O₂ versus 3% O₂ level

Neoplastic and non-neoplastic lesions upon *in vivo* pro-oxidant exposures

To verify whether XPC deficiency also results in an increased sensitivity towards oxidative damage *in vivo*, wild type, *Xpa* and *Xpc* mice (all harboring the *LacZ* gene for mutational analysis) were exposed to pro-oxidative compounds for either 12 weeks (for *LacZ* analyses) or 39 weeks (for histopathological and *LacZ* analyses). Female mice were exposed to DEHP (6,000 ppm, via feed), while male mice were exposed to paraquat (100 ppm, via feed).

Body weight measurements over the duration of exposures demonstrated a decrease in all genotypes for DEHP exposure, while paraquat exposure only had a minor effect on body weight (SI01). Dietary uptake in both exposure groups was comparable to the uptake of the control diet group (SI02).

A

Neoplastic		Control	DEHP
WT	Liver	0%	0%
	Lung	0%	5% (1 adenoma)
XPA	Liver	5% (1 adenoma)	5% (1 adenoma)
	Lung	0%	0%
XPC	Liver	0%	10% (2 carcinomas)
	Lung	5% (1 lymphoma)	0%

B

Non-neoplastic		WT	XPA	XPC
		DEHP	DEHP	DEHP
Liver	Karyomegaly severity	--		-
	Lipofuscin autofluorescence severity	++	+++	+++
	Eosinophilic cytoplasm incidence	+++	+++	+++
	Cholestasis incidence	+++	+++	++
	Glycogenosis incidence		-	---
Kidney	Hydronephrosis incidence	+++	++	+++
	Tubule dilatation incidence	+++	+++	+++
	Scarring severity	+++	+++	+++
	Macrophages incidence	+++	+++	+
		Paraquat	Paraquat	Paraquat
Lung	Septum thickness severity	+++	+	+++
	Peribronchiolar fibrosis severity		+	++
	Lymphoid hyperplasia severity		+	+++
	Inflammatory cells diffuse infiltration severity		+	+++
	Peribronchiolar edema incidence			+

Table 1. Neoplastic and non-neoplastic observations after 39 week pro-oxidant exposure.

A. Neoplastic lesion incidents in percentage per group (n=20), bracketed numbers indicate the number of tumors. None of the tumor incidences are significant when compared to their untreated genotype control ($p < 0.05$). Exposure to paraquat did not result into tumorigenesis.

B. Non-neoplastic changes per group (n=20). (- / + = 10-20%, -- / ++ = 20-30%, --- / +++ = >30% changes relative to the untreated concordant genotype group based on either incidences or averaged ordinal score of severity)

Long-term (39 weeks) exposed mice were analyzed macroscopically during autopsy and afterwards liver, kidney, and lung and eventual gross lesions were subjected to histopathological analyses. The results are summarized in Table 1. In total, few neoplastic lesions (Table 1A) were found after long-term exposure. In the livers of exposed wild type and *Xpa* mice 1 benign tumor (adenoma) for each genotype, but no malignant tumors, were observed. Also one benign tumor (adenoma) was identified in the group of untreated *Xpa* mice. The only malignant liver tumors (2 carcinomas) in the study were observed in the DEHP-treated *Xpc* animals. Also, one malignant tumor (lymphoma) in lung was found in the untreated *Xpc* group. None of the animals (male mice) exposed to paraquat, nor any of their concurrent controls, carried a tumor.

Paraquat exposure had little effect on pathology in liver and kidney. Overall, the response to DEHP was stronger compared to paraquat. Histopathological findings clearly confirmed DEHP exposure in liver and kidney, but no differences between the three genotypes were observed (Table 1B, non-neoplastic findings). Hepatocytes of all DEHP-treated mice diffusely showed eosinophilic cytoplasm consistent with peroxisome proliferation (the most distinct mode of action of DEHP). Furthermore, lipofuscin and cholestasis, indicative for increased oxidative stress, were also apparent. DEHP induced a strong increase in hydronephrosis, tubule dilatation, scarring, and vacuolized and pigmented macrophages in kidney, while paraquat showed no obvious pathology in these two tissues. Even though paraquat was administered through the diet, paraquat induced histopathological lesions in the lungs, especially in *Xpc* mice. For instance, severity of peribronchiolar fibrosis, lymphoid hyperplasia and diffuse infiltration of inflammatory cells were all increased in *Xpc* mice only (Table 1B).

Higher mutational load in Xpc mice due to oxidant exposure

To assess potential differences in sensitivity for oxidative DNA damage between the genotypes we also analyzed the mutational load, as an early tumor risk marker, in the tissues where pathological evidence for exposure and carcinogenesis was found (liver and lung). Mutant frequencies in the *LacZ* gene were measured in both tissues after 12 and 39 weeks of exposure to the pro-oxidants DEHP and paraquat to assess the amount and rate of possible mutation induction due to oxidative stress.

The 12 week exposures to DEHP or paraquat did not result in any significant changes in mutational load in liver or lung of all genotypes compared to the untreated corresponding genotype (Figure 2A). However, the long-term exposure of 39 weeks to both DEHP and paraquat resulted in a statistically significant and exposure-related two-fold increase in mutant frequency in livers of *Xpc* mice only ($p < 0.01$) (Figure 2B). Long-term pro-oxidant exposure did not result in a significantly enhanced mutational load in lung compared to their untreated controls. Mutational loads in the lungs of *Xpc* mice, however, tended to increase faster over time when compared to WT and *Xpa* (Figure 2B). SI03 provides an overview of p -values between all groups.

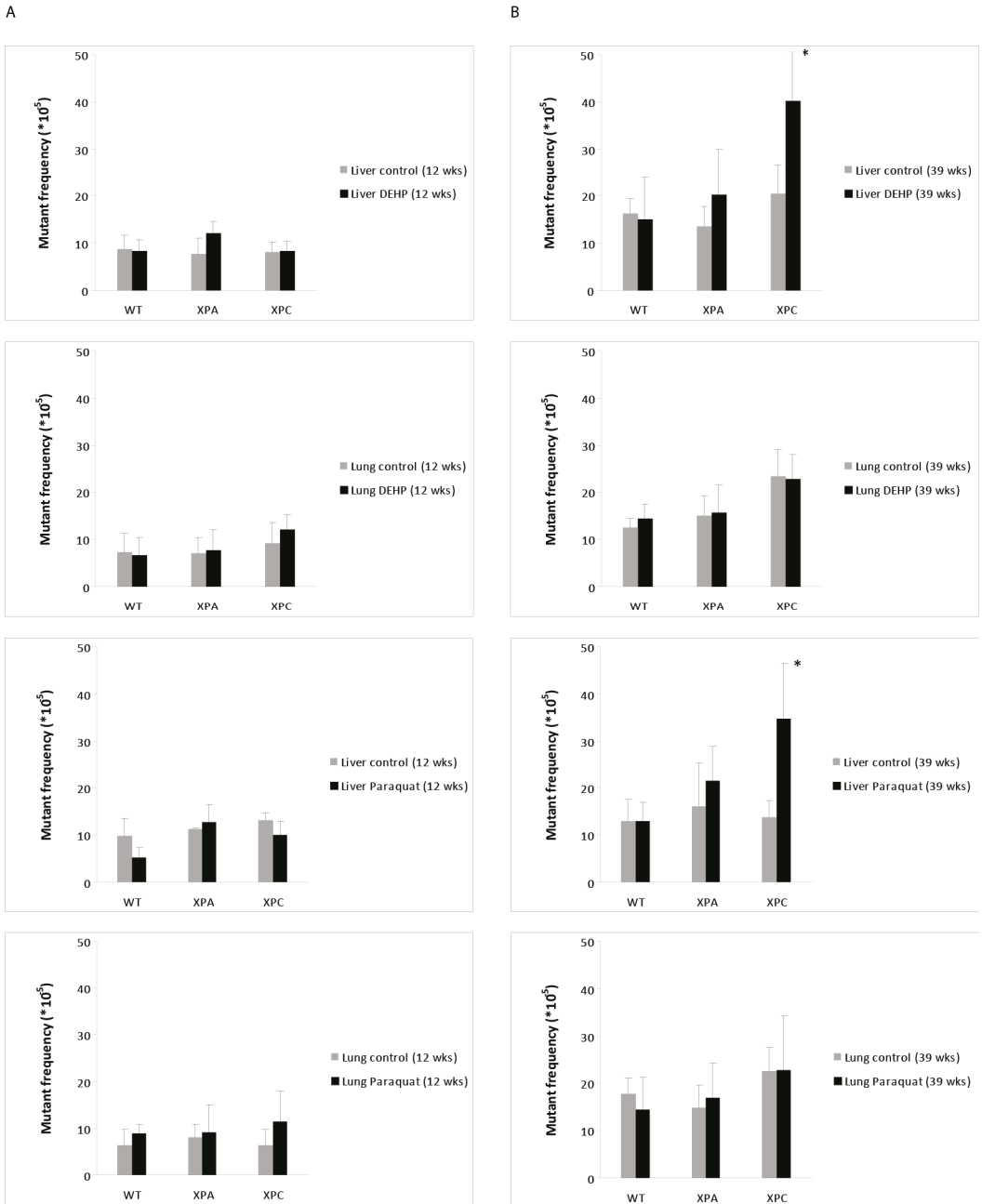


Figure 2. *LacZ* mutant frequencies in liver and lung after pro-oxidant exposure of 12 (A, left column) and 39 weeks (B, right column). Mice were exposed to either DEHP (female mice), paraquat (male mice) or control feed for 39 weeks. * $p < 0.05$ treatment versus control.

Divergent transcriptomic response for glutathione metabolism in Xpc mice

We subsequently attempted to unravel part of the underlying mechanism(s) of the observed increased mutational sensitivity towards oxidative DNA damage in *Xpc* mice by performing genome-wide expression analyses on long-term (39 weeks) DEHP-treated and untreated liver tissue of all three genotypes (GEO database, accession number GSE28296).

The base-line (untreated) transcriptional profiles between the three genotypes were highly similar. One-way analysis of variance (ANOVA) with a False Discovery Rate (FDR) < 0.05 on all untreated samples revealed only 15 differentially expressed genes (DEGs) between the three genotypes, amongst which down regulation of the *Xpa* and *Xpc* gene in their concurrent knockout mouse model (data not shown). These results indicated the basal liver gene expression profiles of the genotypes are similar without exposure.

Subsequently, differences in gene expression in liver upon DEHP exposure were quantified (One-way ANOVA, FDR < 0.05). This analysis revealed 2,278 DEGs in wild type, 3,205 DEGs in *Xpa*, and only 1,449 DEGs in *Xpc* mice. Since these numerical differences could represent a generally higher or lower gene expression level of respectively *Xpa* and *Xpc* (compared to wild type), this could give rise to misleading results. We therefore implemented the following approach to analyze for functional differences between the genotypes. For functional analyses, we used either the DEGs or the top 2,278 genes (ranked on FDR) of each genotype as input. Metacore GeneGO pathway analyses ($p < 0.01$, SI04, data not shown in this thesis) and Gene Ontology (GO) analyses ($p < 0.00001$, SI05, data not shown in this thesis) were performed for both the DEG and the top 2,278 approach. In the latter approach, the wild type differential gene expression profile (2,278 DEGs) was used as a benchmark to ensure more robust results emphasizing the difference between the genotypes. In this approach, for all genotypes the top 2,278 genes (ranked on FDR) was used as input (GEO database, accession number GSE28296). For instance, for *Xpc* it could be the case that the lower number of DEGs is indicative for a lower overall gene expression level. Consequently, many genes did not make the cut-off of FDR < 0.05, resulting in a lack of overrepresented pathways for *Xpc*. So, only if an overrepresented pathway in wild type mice was absent in *Xpc* mice for both types of analyses (DEGs and top 2,278 genes), it was considered as a truly different response from wild type animals.

Using the DEGs and the top 2,278 genes as input for, we screened for functional responses upon pro-oxidant exposure that could explain the observed mutational responses described above. To ensure a more robust pathway analysis we only considered a pathway to be truly regulated if it was generated by both approaches (Overlap results are fully depicted in SI06). The overlap in pathways found with both approaches showed a strong DEHP signature: pathways involved in PPAR regulation of lipid metabolism and fatty acid omega oxidation were up-regulated in all genotypes (Table 2A, SI06) [18-20]. Results of the GO processes corroborated these DEHP exposure-related changes in lipid metabolism (SI05).

Since we were interested in the response and mechanisms behind the observed mutational sensitivity in *Xpc* upon long-term oxidative damage, we examined where *Xpc* mice responded in a significantly different manner from *Xpa* and wild type mice. For this, we used GeneGO pathway analyses. *Xpc* specific pathways (Table 2B & SI06) regulated in both approaches (DEGs and top 2,278 genes as input) were amongst others a down-regulation in nitrogen and glycine, serine, cysteine and threonine

metabolism and also an up-regulation of cell DNA replication in early S phase. Reciprocally, pathways regulated in both wild type and *Xpa*, but not in *Xpc* (Table 2B) included a significant up-regulation of glutathione metabolism, apoptosis-related BAD phosphorylation and spindle assembly and chromosome separation, plus down-regulated aldosterone-mediated regulation of epithelial sodium channel sodium transport.

A. Pathways differentially regulated in all genotypes

GeneGO p<0.01 in WT & XPA & XPC	Regulation
Regulation of lipid metabolism_PPAR regulation of lipid metabolism	up
Fatty Acid Omega Oxidation	up
Cell adhesion_Plasmin signaling	down
Blood coagulation_Blood coagulation	down
Immune response_Lectin induced complement pathway	down
Cytoskeleton remodeling_TGF, WNT and cytoskeletal remodeling	mix
Cytoskeleton remodeling_Cytoskeleton remodeling	mix
Atherosclerosis_Role of ZNF202 in regulation of expression of genes involved in Atherosclerosis	mix


B. Pathways differentially regulated between WT+XPA versus XPC

GeneGO p<0.01 only in WT & XPA	Regulation
Glutathione metabolism / Rodent version	up
Apoptosis and survival_BAD phosphorylation	up
Cell cycle_Spindle assembly and chromosome separation	up
Transport_Aldosterone-mediated regulation of ENaC sodium transport	down
GeneGO p<0.01 only in XPC	Regulation
Cell cycle_Start of DNA replication in early S phase	up
Nitrogen metabolism/ Rodent version	down
Glycine, serine, cysteine and threonine metabolism	down
Development_Mu-type opioid receptor signaling via Beta-arrestin	down

Table 2. GeneGO pathway overlap (DEGs and top2278 genes input, $p < 0.01$)

Other research groups have implicated XPC functionality in base excision repair (BER), redox homeostasis and cell cycle regulation (overview in [21]). Therefore, we also assessed these responses in more detail at single gene level. All genes that have previously been associated with XPC functionality in literature (listed in Table 3A) appeared not to be differentially regulated on transcriptional level in our current study, and if so, no clear difference between the three genotypes was observed. One gene that is involved in BER and redox homeostasis [22] was slightly differentially regulated in *Xpc* mice compared to *Xpa* and wild type mice: *Apex1* was up-regulated in *Xpa* and wild type (1.6 and 1.4 times respectively), and less in *Xpc* (1.2). Additionally, *Nrf1* (*NFE2L1*) was up-regulated in wild type (1.4) and only 1.2 times in *Xpa* and *Xpc*.

A.					
Reference	Gene	WT DEHP-Control	XPA DEHP-Control	XPC DEHP-Control	Process
D'Errico et al. 2006	Ogg1	1.02	-1.02	-1.02	BER
Shimizu et al. 2003, 2010	TDG	1.24	1.10	1.06	BER
Shimizu et al. 2010	SMUG1	1.01	-1.02	-1.03	BER
Meira et al. 2001	Apex	1.63	1.39	1.24	BER/Redox
Wang et al. 2003, 2004	p53	1.00	1.00	1.02	Cell cycle
Colton et al. 2006	ATM	1.00	-1.02	-1.01	Cell cycle
Auclair et al. 2003, 2004	ATR	1.29	1.41	1.27	Cell cycle
Ray et al. 2009	SNF5 (Smarb1)	1.28	1.11	1.14	Cell cycle
Rezvani et al. 2011	DNAPK (Prkdc)	1.18	1.04	1.15	DNA damage/Redox
Rezvani et al. 2011	NOX1	1.05	-1.03	-1.01	Redox
Rezvani et al. 2011	AKT1	-1.07	1.01	-1.09	Redox
Han et al. 2012	Nrf1 (NFE2L1)	1.36	1.15	1.15	Glutathione metabolism
Liu et al. 2011, Langie et al. 2007	Overall process, no specific gene	-	-	-	Glutathione metabolism
B.					
Melis et al. 2012	SQSTM1	1.79	1.55	1.19	Antioxidant response/Glutathione
Genes involved in glutathione metabolism	GSTA1	3.72	2.40	1.86	Glutathione metabolism
	GSTA2	2.85	1.52	1.45	Glutathione metabolism
	GSTA4	1.37	1.32	1.03	Glutathione metabolism
	GSTK1	1.24	1.06	1.11	Glutathione metabolism
	GSTM1	1.96	1.87	1.35	Glutathione metabolism
	GSTM2	1.17	-1.02	1.03	Glutathione metabolism
	GSTM3	4.31	4.12	2.04	Glutathione metabolism
	GSTM4	2.54	1.83	1.88	Glutathione metabolism
	GSTM5	1.07	1.03	-1.02	Glutathione metabolism
	GSTM6	1.44	1.01	1.08	Glutathione metabolism
	GSTM7	1.08	-1.12	-1.16	Glutathione metabolism
	GSTO1	1.10	-1.02	1.06	Glutathione metabolism
	GSTO2	1.00	-1.08	-1.03	Glutathione metabolism
	GSTP1	2.88	2.85	2.11	Glutathione metabolism
	GSTP2	2.77	2.82	2.20	Glutathione metabolism
	GSTT1	-1.05	-1.13	-1.12	Glutathione metabolism
	GSTT2	1.68	2.08	1.81	Glutathione metabolism
	GSTT3	1.11	-1.20	-1.22	Glutathione metabolism
	GSTT4	-1.01	1.02	-1.04	Glutathione metabolism
	GSTCD	1.11	-1.03	-1.02	Glutathione metabolism
	GSTZ1	-1.15	-1.19	-1.23	Glutathione metabolism
	GPX1	1.37	1.22	1.12	Glutathione metabolism
	GPX2	1.44	1.26	1.42	Glutathione metabolism
	GPX3	1.13	1.21	1.15	Glutathione metabolism
	GPX4	1.44	1.34	1.30	Glutathione metabolism
	GPX5	1.01	-1.03	-1.06	Glutathione metabolism
	GPX6	-1.49	-1.71	-1.24	Glutathione metabolism
	GPX7	1.54	1.70	1.47	Glutathione metabolism
	GPX8	1.01	-1.01	1.07	Glutathione metabolism
	Mgst1	1.28	1.01	1.14	Glutathione metabolism
	Mgst2	-1.14	-1.01	1.05	Glutathione metabolism
	Mgst3	1.61	1.62	1.37	Glutathione metabolism
	GSR	1.61	1.32	1.23	Glutathione metabolism
	GSS	1.26	1.29	1.06	Glutathione metabolism
	GCLC	2.33	1.31	1.50	Glutathione metabolism
	CTH (CGL)	-1.15	-1.45	-1.84	Glutathione metabolism
	CBS	-1.38	-1.41	-2.04	Glutathione metabolism
	Oplah	1.85	1.88	1.59	Glutathione metabolism
	Anpep	1.28	1.29	1.25	Glutathione metabolism



■ Xpc < WT and Xpa
■ Xpc < WT or Xpa
■ Xpc > WT and Xpa

Table 3. XPC-related functionality.

A. Genes and process (fold changes (DEHP vs control)) implicated with additional XPC functionality
B. Fold changes of genes involved in glutathione metabolism (DEHP vs control)

Previous *in vitro* studies also showed that XPC deficiency resulted in an affected glutathione metabolism [10;23;24]. In our 9 month *in vivo* study, the glutathione metabolism and related pathways (nitrogen metabolism and glycine, serine, cysteine and threonine metabolism) revealed a different transcriptional response in *Xpc* compared to both wild type and *Xpa*. Besides pathway analysis we also looked at the expression data of single genes known to be involved in glutathione metabolism (Table 3B). At the gene expression level, *Xpc* mice appeared to be less responsive in comparison to *Xpa* and wild type mice since the majority of these genes showed a lower fold change in *Xpc* mice. Another less responsive gene in *Xpc* is p62/SQSTM1 (Table 3B), which is part of the TFIIH complex, but is also involved in antioxidant response functioning. The XPC protein contains two binding domains for p62, one of them overlapping with the binding site of BER protein OGG1 [1]. In our study on transcriptional

level, p62/SQSTM1 was differentially up-regulated in both wild type (1.8) and *Xpa* (1.6), but less in *Xpc* (1.2) (Table 3B).

Discussion

We, and others, hypothesized that XPC is involved in the prevention or removal of oxidative DNA damage by functionality outside of NER [6-10;17;21;23;25-28]. *Xpc* deficiency therefore could lead to more DNA damage as a consequence of their reduced capability to cope with oxidative stress. This could explain the observed increase in lung tumor incidence and corresponding increase in mutational load in *Xpc* mice compared to wild type and *Xpa* mice [17]. *Xpc* mice revealed an increase in lung and liver tumors, while in *Xpa* mice only liver tumor incidence was increased at final autopsy compared to wild type mice. Hollander et al. also showed an enhanced lung tumor incidence in *Xpc* mice [29]. Our previous study also demonstrated a decreased survival of *Xpc* MEFs upon normoxic versus atmospheric oxygen exposure in comparison to *Xpa* and wild type cells.

We assessed if the decreased survival response exhibited in *Xpc* MEFs was correlated to an increase in mutations using different oxygen exposure levels. Our results demonstrated that *Xpc* cells are specifically more sensitive towards oxidative DNA damage when compared to wild type and *Xpa* cells. Others have also previously implicated XPC in the prevention or removal of oxidative DNA damage *in vitro* using exposures to oxidative stressors [6-10;23;25-28]. It was however still unclear if, and at what rate, XPC deficiency contributes to the level of oxidative DNA damage *in vivo*. Therefore, we exposed *Xpa*, *Xpc* and wild type mice to the well-known pro-oxidants DEHP and paraquat through the diet and measured several parameters after a 12 week and a 39 week exposure to these compounds.

Histopathological analyses showed only a minor or no response in tumor formation after 39-week exposure to the low potent carcinogen DEHP or non-carcinogen paraquat, respectively. Paraquat does not induce tumors in rodents (EPA database, <http://www.epa.gov/iris/subst/0183.htm>, 2012) and exposure in the present study also did not lead to significant tumor formation in all three genotypes tested. The only malignant tumors observed in our current studies were found in *Xpc* mice. DEHP is carcinogenic to mice in a classical 2-year rodent bioassay at a dose of 6,000 ppm [18]. Apparently, shorter exposure times do not lead to a significant tumor response in mice, not even in the DNA repair-deficient models *Xpa* and *Xpc*. This finding is in line with our previous results in wild type and *Xpa* mice [30].

DEHP induced oxidative stress in liver since increased levels of lipofuscin and cholestasis [31-33] were found in exposed animals of all three genotypes. The effect of paraquat on histopathology in the liver was only marginal (data not shown), but did show a genotypical difference in *Xpc* lings.

Since we expected that pro-oxidant exposure would enhance oxidative DNA-damaging events, we tested whether *Xpc* mice accumulated more mutations due to the exposure of DEHP and paraquat. *LacZ* mutant frequency analyses demonstrated a significant increase in mutational load after pro-oxidant exposure in livers of *Xpc* mice only. This increase however was only detected after 39 weeks of exposure. At 12 weeks of pro-oxidant exposure no significant increase the mutational load in any of the genotypes was observed. In lung, *LacZ* mutant frequency analyses did not show any DEHP or paraquat exposure-related effect. However, *LacZ* mutant frequencies were higher in lung of all female and male *Xpc* mice, most likely due to oxygen exposure. The mutational load of these 1 year old mice

(age of the mice after 39 weeks of exposure) is comparable to previous studies with C57BL/6J mice at that age [17].

Since XPC and XPA are both part of NER, the increases in mutational load after DEHP, paraquat and oxygen exposure implicates that the XPC protein has additional functionality outside NER, which appears to be involved in the prevention or the removal of oxidative DNA damage. The fact that mutant frequencies were only affected after 39 weeks of DEHP exposure and not after 12 weeks suggests a slow accumulation of mutations upon oxidative stress in *Xpc* mice. This could be due to either the relatively slow cell division in adult livers or to an additional function of XPC that involves a mechanism which prevents oxidative DNA damage accumulation in a time-related manner.

Using microarray analyses we set out to elucidate the underlying differences between *Xpa* and *Xpc* sensitivity *in vivo* towards mutation accumulation and consequential divergent tumor response. DEHP exposure-related effects [18;34;35] in liver of all three genotypes were apparent, in particular the disturbed regulation of lipid and fatty acid metabolism was distinct.

XPC functionality outside of NER has been implied in base excision repair [6;8;9;28]. In this study, no convincing transcriptional evidence was found implicating supplemental functionality of XPC in base excision repair. However, epigenetic factors, post-translational modifications and protein interactions could be responsible for these previously proposed interactions and effects. Concerning these protein interactions, our gene expression data indicated that Nrf2-target and antioxidant enhancer p62/SQSTM1 was up-regulated in both wild type and *Xpa* mice, but less in *Xpc* mice. The XPC protein holds two binding sites for p62/SQSTM1 interaction. A recent study pointed out that p62/SQSTM1 plays a critical role in an oxidative stress response pathway by its direct interaction with the ubiquitin ligase adaptor Kelch-like ECH-associated protein 1 (KEAP1), resulting in constitutive activation of the transcription factor NRF2 [36]. P62/SQSTM1 contributes to activation of NRF2 target genes in response to oxidative stress through creating a positive feedback loop [37]. Since the XPC protein contains binding sites for interaction with p62/SQSTM1, the loss of XPC could cause a disturbed oxidative DNA damage signaling resulting in a lower antioxidant (glutathione) response. Decreased p62/SQSTM1 transcript and protein levels by siRNA silencing have been correlated to a decrease in glutathione levels [38], which is in line with our current *in vivo* observations.

The divergent glutathione response and related pathways like nitrogen and cysteine metabolism were, despite the substantial DEHP-related gene expression signature and an overall comparable response between the three genotypes, one of the most interesting and distinct differences observed between on the one hand *Xpc* and on the other hand both *Xpa* and wild type. After exposure to DEHP, one expects a sufficient induction of antioxidant defense systems to cope with the increased oxidative stress levels [39-41]. One of the key players in such an antioxidant response is the glutathione metabolism [42-45]. Glutathione scavenges harmful molecules such as electrophiles and reactive oxygen species, thereby inhibiting or preventing DNA damage [46]. At the pathway level, glutathione metabolism and amino acid metabolism involved in this process were indeed significantly up-regulated in both wild type and *Xpa* mice upon long-term DEHP exposure, but these responses were not significantly affected in *Xpc* mice. Additionally, the p62/SQSTM1 gene and a multitude of genes involved in glutathione response were less responsive in *Xpc* [36]. Very recently, glutathione homeostasis was also directly linked to XPC functionality *in vitro*, since *Nrf1* regulates *Xpc* expression and subsequent DNA damage repair through maintaining GSH levels [23]. Moreover, reduced

glutathione levels and a subsequent imbalanced redox status were demonstrated in *Xpc* silenced cells [10]. *In vitro*, interplay between NER and glutathione antioxidant response was previously suggested [24]. We subsequently attempted to measure glutathione-related biological parameters in the long-term exposed liver samples, but were unfortunately not able to reliably establish a clear difference between the three genotypes using these tissues. This could be explained by either the multiple freeze-thaw cycles the samples underwent prior to these analyses or by the possibility that the differences are only subtle *in vivo* considering the fact that the mutational load also increased slowly over time.

Taken together, our current results and the growing number of data published by others suggest an affected redox status in XPC-deficient mice and cells, which may contribute to the observed increased levels of oxidative DNA damage in our study. Some bulky oxidative DNA lesions might remain unrepaired by a deficient NER in both *Xpc* and *Xpa* cells [47,48]. In *Xpc* mice, an insufficient antioxidant response in combination with a possibly affected BER (XPC also contains a binding site for BER protein OGG1) appears to result into an increased sensitivity towards oxidative DNA damage. Our results additionally indicate that this is a slowly accumulating process *in vivo* and has therefore probably not been observed *in vivo* before.

Conflict of interest

Authors declare there is no conflict of interest.

Acknowledgements

We thank the Animal Facilities of the Netherlands Vaccine Institute (NVI) and the MicroArray Department Amsterdam for their skillful support. We also thank Prof. Dr. Errol Friedberg for providing us with the *Xpc* mouse model. The work presented here was in part financially supported by NIH/NIEHS (Comparative Mouse Genomics Centers Consortium) Grant 1U01 ES11044 and by STW Grant STW-LGC.6935.

Supplemental information

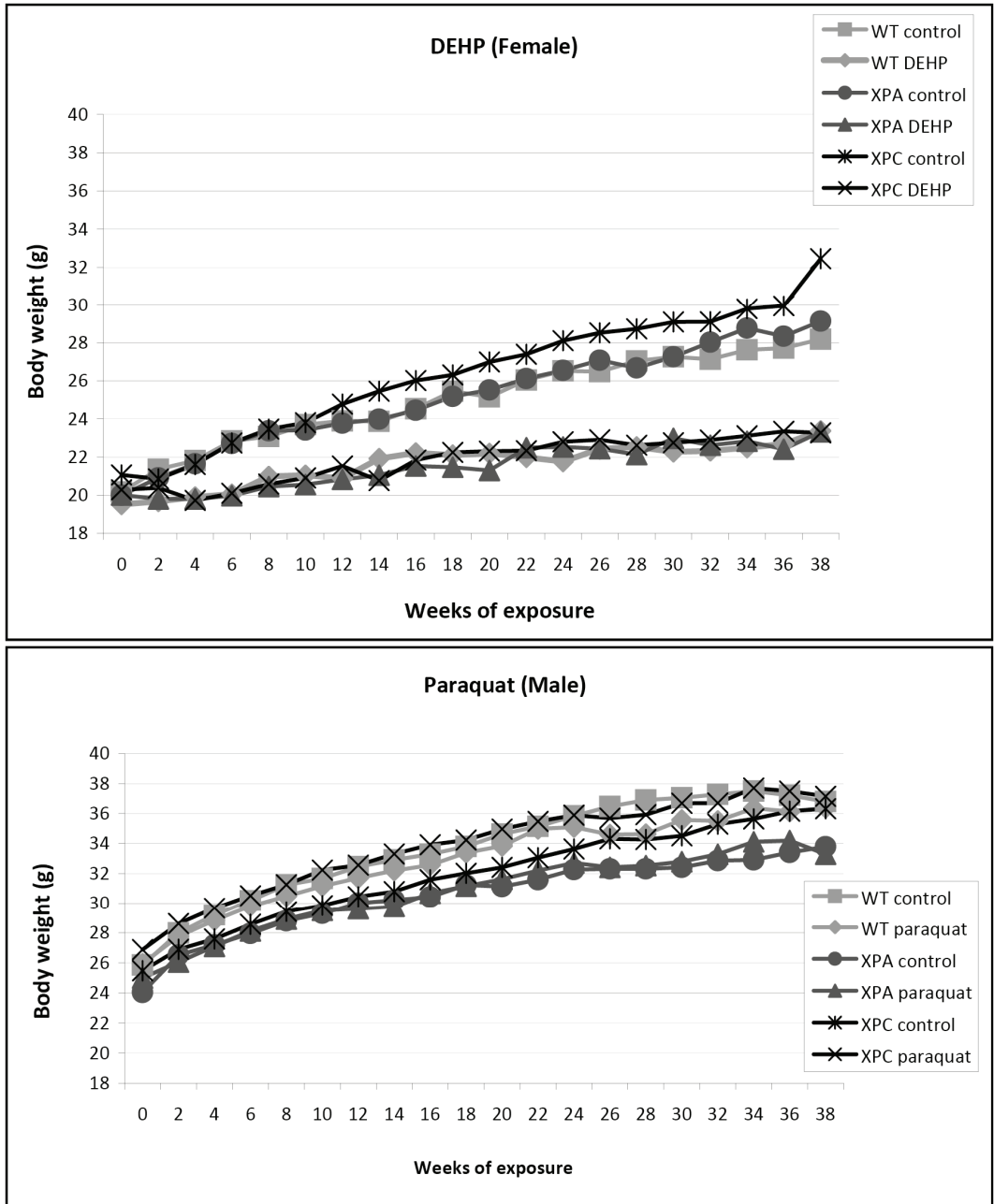
Supplementary information is available at the journal's website. Complete raw and normalized microarray data and their MIAME compliant metadata have been deposited at GEO (www.ncbi.nlm.nih.gov/geo) under accession number GSE28296.

Reference List

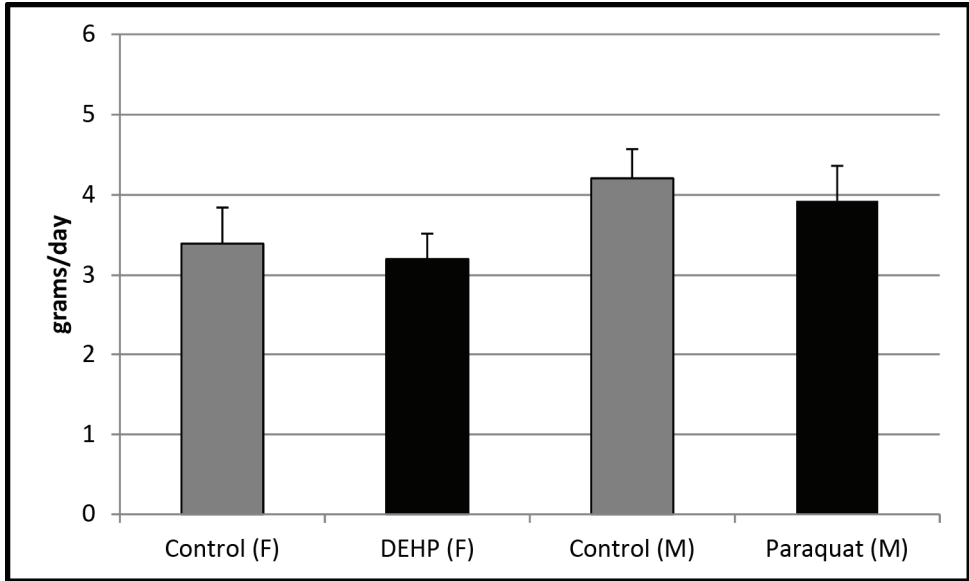
- [1] J.E.Cleaver, E.T.Lam, I.Revet. Disorders of nucleotide excision repair: the genetic and molecular basis of heterogeneity, *Nat.Rev.Genet.*, 10, (2009) 756-768.
- [2] A.Y.Maslov, J.Vijg. Genome instability, cancer and aging, *Biochim.Biophys.Acta*, 1790, (2009) 963-969.
- [3] E.C.Friedberg, G.C.Walker, W.Siede, R.D.Wood, R.A.Schultz, T.Ellenberger. *DNA Repair and Mutagenesis*, ASM Press, 2006.
- [4] M.Dizdaroglu. Base-excision repair of oxidative DNA damage by DNA glycosylases, *Mutat.Res.*, 591, (2005) 45-59.
- [5] B.van Loon, E.Markkanen, U.Hubscher. Oxygen as a friend and enemy: How to combat the mutational potential of 8-oxo-guanine, *DNA Repair (Amst)*, 9, (2010) 604-616.
- [6] S.N.Kassam, A.J.Rainbow. Deficient base excision repair of oxidative DNA damage induced by methylene blue plus visible light in xeroderma pigmentosum group C fibroblasts, *Biochem.Biophys.Res.Communic.*, 359, (2007) 1004-1009.
- [7] Y.Okamoto, P.H.Chou, S.Y.Kim, N.Suzuki, Y.R.Laxmi, K.Okamoto, X.Liu, T.Matsuda, S.Shibutani. Oxidative DNA damage in XPC-knockout and its wild mice treated with equine estrogen, *Chem.Res.Toxicol.*, 21, (2008) 1120-1124.
- [8] M.D'Errico, E.Parlanti, M.Teson, B.M.de Jesus, P.Degan, A.Calcagnile, P.Jaruga, M.Bjoras, M.Crescenzi, A.M.Pedrini, J.M.Egly, G.Zambruno, M.Stefanini, M.Dizdaroglu, E.Dogliotti. New functions of XPC in the protection of human skin cells from oxidative damage, *EMBO J.*, 25, (2006) 4305-4315.
- [9] Y.Shimizu, S.Iwai, F.Hanaoka, K.Sugasawa. Xeroderma pigmentosum group C protein interacts physically and functionally with thymine DNA glycosylase, *EMBO J.*, 22, (2003) 164-173.
- [10] S.Y.Liu, C.Y.Wen, Y.J.Lee, T.C.Lee. XPC silencing sensitizes glioma cells to arsenic trioxide via increased oxidative damage, *Toxicol.Sci.*, 116, (2010) 183-193.
- [11] P.J.Brooks, D.S.Wise, D.A.Berry, J.V.Kosmoski, M.J.Smerdon, R.L.Somers, H.Mackie, A.Y.Spoonde, E.J.Ackerman, K.Coleman, R.E.Tarone, J.H.Robbins. The oxidative DNA lesion 8,5'-(S)-cyclo-2'-deoxyadenosine is repaired by the nucleotide excision repair pathway and blocks gene expression in mammalian cells, *J.Biol.Chem.*, 275, (2000) 22355-22362.
- [12] K.H.Kraemer, M.M.Lee, J.Scotto. DNA repair protects against cutaneous and internal neoplasia: evidence from xeroderma pigmentosum, *Carcinogenesis*, 5, (1984) 511-514.
- [13] K.H.Kraemer, M.M.Lee, J.Scotto. Xeroderma pigmentosum. Cutaneous, ocular, and neurologic abnormalities in 830 published cases, *Arch.Dermatol.*, 123, (1987) 241-250.
- [14] K.H.Kraemer. Sunlight and skin cancer: another link revealed, *Proc.Natl.Acad.Sci.U.S.A.*, 94, (1997) 11-14.
- [15] P.C.Hanawalt, J.M.Ford, D.R.Lloyd. Functional characterization of global genomic DNA repair and its implications for cancer, *Mutat.Res.*, 544, (2003) 107-114.
- [16] T.Yasuda, K.Sugasawa, Y.Shimizu, S.Iwai, T.Shiomi, F.Hanaoka. Nucleosomal structure of undamaged DNA regions suppresses the non-specific DNA binding of the XPC complex, *DNA Repair (Amst)*, 4, (2005) 389-395.
- [17] J.P.Melis, S.W.Wijnhoven, R.B.Beems, M.Roodbergen, B.J.van den, H.Moon, E.Friedberg, G.T.van der Horst, J.H.Hoeijmakers, J.Vijg, H.van Steeg. Mouse models for xeroderma pigmentosum group A and group C show divergent cancer phenotypes, *Cancer Res.*, 68, (2008) 1347-1353.
- [18] R.M.David, M.R.Moore, D.C.Finney, D.Guest. Chronic toxicity of di(2-ethylhexyl)phthalate in mice, *Toxicol.Sci.*, 58, (2000) 377-385.
- [19] H.Yamashita, A.Itsuki, M.Kimoto, M.Hiemori, H.Tsuji. Acetate generation in rat liver mitochondria; acetyl-CoA hydrolase activity is demonstrated by 3-ketoacyl-CoA thiolase, *Biochim.Biophys.Acta*, 1761, (2006) 17-23.
- [20] C.C.Willhite. Weight-of-evidence versus strength-of-evidence in toxicologic hazard identification: Di(2-ethylhexyl)phthalate (DEHP), *Toxicology*, 160, (2001) 219-226.

- [21] J.P.Melis, M.Luijten, L.H.Mullenders, H.van Steeg. The role of XPC: implications in cancer and oxidative DNA damage, *Mutat.Res.*, 728, (2011) 107-117.
- [22] L.B.Meira, A.M.Reis, D.L.Cheo, D.Nahari, D.K.Burns, E.C.Friedberg. Cancer predisposition in mutant mice defective in multiple genetic pathways: uncovering important genetic interactions, *Mutat.Res.*, 477, (2001) 51-58.
- [23] W.Han, M.Ming, R.Zhao, J.Pi, C.Wu, Y.Y.He. The Nrf1 CNC-bZIP protein promotes cell survival and nucleotide excision repair through maintaining glutathione homeostasis, *J.Biol.Chem.*, (2012).
- [24] S.A.Langie, A.M.Knaapen, J.M.Houben, F.C.van Kempen, J.P.de Hoon, R.W.Gottschalk, R.W.Godschalk, F.J.van Schooten. The role of glutathione in the regulation of nucleotide excision repair during oxidative stress, *Toxicol.Lett.*, 168, (2007) 302-309.
- [25] R.Abbasi, T.Efferth, C.Kuhmann, T.Opatz, X.Hao, O.Popanda, P.Schmezer. The endoperoxide ascaridol shows strong differential cytotoxicity in nucleotide excision repair-deficient cells, *Toxicol.Appl.Pharmacol.*, 259, (2012) 302-310.
- [26] H.R.Rezvani, R.Rossignol, N.Ali, G.Benard, X.Tang, H.S.Yang, T.Jouary, H.de Verneuil, A.Taieb, A.L.Kim, F.Mazurier. XPC silencing in normal human keratinocytes triggers metabolic alterations through NOX-1 activation-mediated reactive oxygen species, *Biochim.Biophys.Acta*, 1807, (2011) 609-619.
- [27] H.R.Rezvani, A.L.Kim, R.Rossignol, N.Ali, M.Daly, W.Mahfouf, N.Bellance, A.Taieb, H.de Verneuil, F.Mazurier, D.R.Bickers. XPC silencing in normal human keratinocytes triggers metabolic alterations that drive the formation of squamous cell carcinomas, *J.Clin.Invest*, 121, (2011) 195-211.
- [28] Y.Shimizu, Y.Uchimura, N.Dohmae, H.Saitoh, F.Hanaoka, K.Sugasawa. Stimulation of DNA Glycosylase Activities by XPC Protein Complex: Roles of Protein-Protein Interactions, *J.Nucleic Acids*, 2010, (2010).
- [29] M.C.Hollander, R.T.Philburn, A.D.Patterson, S.Velasco-Miguel, E.C.Friedberg, R.I.Linnoila, A.J.Fornace, Jr. Deletion of XPC leads to lung tumors in mice and is associated with early events in human lung carcinogenesis, *Proc.Natl.Acad.Sci.U.S.A.*, 102, (2005) 13200-13205.
- [30] A.Mortensen, M.Bertram, V.Aarup, I.K.Sorensen. Assessment of carcinogenicity of di(2-ethylhexyl)phthalate in a short-term assay using *Xpa*^{-/-} and *Xpa*^{-/-}/*p53*^{+/-} mice, *Toxicol.Pathol.*, 30, (2002) 188-199.
- [31] R.S.Sohal, U.T.Brunk. Lipofuscin as an indicator of oxidative stress and aging, *Adv.Exp.Med.Biol.*, 266, (1989) 17-26.
- [32] T.Jung, A.Hohn, T.Grune. Lipofuscin: detection and quantification by microscopic techniques, *Methods Mol.Biol.*, 594, (2010) 173-193.
- [33] M.M.Tiao, T.K.Lin, P.W.Wang, J.B.Chen, C.W.Liou. The role of mitochondria in cholestatic liver injury, *Chang Gung.Med.J.*, 32, (2009) 346-353.
- [34] H.Yamashita, A.Itsuki, M.Kimoto, M.Hiemori, H.Tsuji. Acetate generation in rat liver mitochondria; acetyl-CoA hydrolase activity is demonstrated by 3-ketoacyl-CoA thiolase, *Biochim.Biophys.Acta*, 1761, (2006) 17-23.
- [35] C.C.Willhite. Weight-of-evidence versus strength-of-evidence in toxicologic hazard identification: Di(2-ethylhexyl)phthalate (DEHP), *Toxicology*, 160, (2001) 219-226.
- [36] I.P.Nezis, H.Stenmark. p62 at the Interface of Autophagy, Oxidative Stress Signaling, and Cancer, *Antioxid.Redox.Signal.*, (2012).
- [37] A.Jain, T.Lamark, E.Sjottem, K.B.Larsen, J.A.Awuh, A.Overvatn, M.McMahon, J.D.Hayes, T.Johansen. p62/SQSTM1 is a target gene for transcription factor NRF2 and creates a positive feedback loop by inducing antioxidant response element-driven gene transcription, *J.Biol.Chem.*, 285, (2010) 22576-22591.
- [38] I.M.Copple, A.Lister, A.D.Obeng, N.R.Kitteringham, R.E.Jenkins, R.Layfield, B.J.Foster, C.E.Goldring, B.K.Park. Physical and functional interaction of sequestosome 1 with Keap1 regulates the Keap1-Nrf2 cell defense pathway, *J.Biol.Chem.*, 285, (2010) 16782-16788.
- [39] J.Limon-Pacheco, M.E.Gonsebatt. The role of antioxidants and antioxidant-related enzymes in protective responses to environmentally induced oxidative stress, *Mutat.Res.*, 674, (2009) 137-147.

- [40] W.O.Osburn, T.W.Kensler. Nrf2 signaling: an adaptive response pathway for protection against environmental toxic insults, *Mutat.Res.*, 659, (2008) 31-39.
- [41] J.D.Hayes, L.I.McLellan. Glutathione and glutathione-dependent enzymes represent a co-ordinately regulated defence against oxidative stress, *Free Radic.Res.*, 31, (1999) 273-300.
- [42] K.P.Economopoulos, T.N.Sergentanis. GSTM1, GSTT1, GSTP1, GSTA1 and colorectal cancer risk: a comprehensive meta-analysis, *Eur.J.Cancer*, 46, (2010) 1617-1631.
- [43] K.W.Kang, S.J.Lee, S.G.Kim. Molecular mechanism of nrf2 activation by oxidative stress, *Antioxid.Redox.Signal.*, 7, (2005) 1664-1673.
- [44] K.A.Jung, M.K.Kwak. The Nrf2 system as a potential target for the development of indirect antioxidants, *Molecules.*, 15, (2010) 7266-7291.
- [45] E.Laborde. Glutathione transferases as mediators of signaling pathways involved in cell proliferation and cell death, *Cell Death.Differ.*, 17, (2010) 1373-1380.
- [46] R.Franco, J.A.Cidlowski. Apoptosis and glutathione: beyond an antioxidant, *Cell Death.Differ.*, 16, (2009) 1303-1314.
- [47] K.Randerath, E.Randerath, C.V.Smith, J.Chang. Structural origins of bulky oxidative DNA adducts (type II I-compounds) as deduced by oxidation of oligonucleotides of known sequence, *Chem.Res.Toxicol.*, 9, (1996) 247-254.
- [48] Y.Wang. Bulky DNA lesions induced by reactive oxygen species, *Chem.Res.Toxicol.*, 21, (2008) 276-281.
- [49] M.E.Dolle, H.Giese, C.L.Hopkins, H.J.Martus, J.M.Hausdorff, J.Vijg. Rapid accumulation of genome rearrangements in liver but not in brain of old mice, *Nat.Genet.*, 17, (1997) 431-434.
- [50] S.W.Wijnhoven, H.J.Kool, L.H.Mullenders, R.Slater, A.A.van Zeeland, H.Vrieling. DMBA-induced toxic and mutagenic responses vary dramatically between NER-deficient Xpa, Xpc and Csb mice, *Carcinogenesis*, 22, (2001) 1099-1106.
- [51] D.L.Cheo, H.J.Ruven, L.B.Meira, R.E.Hammer, D.K.Burns, N.J.Tappe, A.A.van Zeeland, L.H.Mullenders, E.C.Friedberg. Characterization of defective nucleotide excision repair in XPC mutant mice, *Mutat.Res.*, 374, (1997) 1-9.
- [52] A.de Vries, H.van Steeg. Xpa knockout mice, *Semin.Cancer Biol.*, 7, (1996) 229-240.
- [53] J.L.A.Pennings, Wendy Rodenburg, Sandra Imholz, Maria P.H.Koster, Conny T.M.van Oostrom, Timo M.Breit, Peter C.J.I.Schielen, Annemieke de Vries. Gene Expression Profiling in a Mouse Model Identifies Fetal Liver- and Placenta-Derived Potential Biomarkers for Down Syndrome Screening, *PLoS ONE*, 6, (2011) e18866.



Supplemental information 1. Body weight curves. Body weight curves of all three genotypes during either pro-oxidant exposure or control feed.

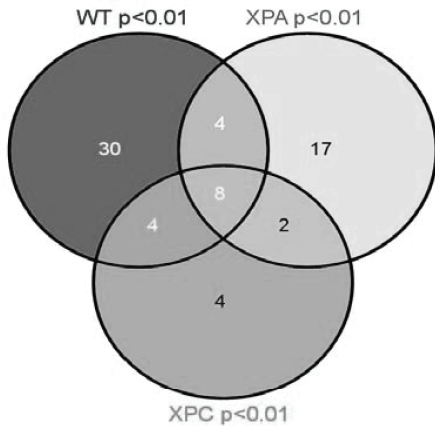


Supplemental information 2. Average daily food uptake per mouse per exposure group. Food uptake was monitored in 6 cages per per exposure (2 of each genotype) for 5 weeks. Uptake between the genotypes was comparable for all food types. (F) = female mice, (M) = male mice.

Liver			Lung		
DEHP	WT control vs XPA control	p = 0.2530	DEHP	WT control vs XPA control	p = 0.2663
	WT control vs XPC control	p = 0.1534		WT control vs XPC control	p = 0.0043
	XPA control vs XPC control	p = 0.0426		XPA control vs XPC control	p = 0.0321
	WT dehp vs XPA dehp	p = 0.3589		WT DEHP vs XPA DEHP	p = 0.6722
	WT dehp vs XPC dehp	p = 0.0012		WT DEHP vs XPC DEHP	p = 0.0142
	XPA dehp vs XPC dehp	p = 0.0062		XPA DEHP vs XPC DEHP	p = 0.0743
Paraquat	WT control vs XPA control	p = 0.4666	Paraquat	WT control vs XPA control	p = 0.4944
	WT control vs XPC control	p = 0.7304		WT control vs XPC control	p = 0.2215
	XPA control vs XPC control	p = 0.5755		XPA control vs XPC control	p = 0.0219
	WT paraquat vs XPA paraquat	p = 0.0291		WT Paraquat vs XPA Paraquat	p = 0.2603
	WT Paraquat vs XPC Paraquat	p = 0.0014		WT Paraquat vs XPC Paraquat	p = 0.0479
	XPA Paraquat vs XPC Paraquat	p = 0.0406		XPA Paraquat vs XPC Paraquat	p = 0.1503

Supplemental information 3. Additional information to figure 2. All group t-test comparisons, *p*-values after 39 weeks of pro-oxidant exposure. *P*-values < 0.01 are indicated in bold

Supplemental information 6. Venn diagram of distribution of all GeneGO pathways generated by top 2278 significant genes and DEGs. Pathways that were considered to be truly regulated (yielded by both the DEGs and the top 2278 genes as Metacore input) were used in the overlap analysis (Venn diagram) shown here. Table 2 shows a selection of the fields of this Venn distribution.



Common elements in "WTp0.01", "XPAp0.01" and "XPCp0.01" (8 pathways)

Regulation of lipid metabolism_PPAR regulation of lipid metabolism
 Cytoskeleton remodeling_TGF, WNT and cytoskeletal remodeling
 Cytoskeleton remodeling_Cytoskeleton remodeling
 Fatty Acid Omega Oxidation
 Cell adhesion_Plasmin signaling
 Atherosclerosis_Role of ZNF202 in regulation of expression of genes involved in Atherosclerosis
 Blood coagulation_Blood coagulation
 Immune response_Lectin induced complement pathway

Common elements in "WTp0.01" and "XPAp0.01" (4 pathways)

Apoptosis and survival_BAD phosphorylation
 Glutathione metabolism / Rodent version
 Cell cycle_Spindle assembly and chromosome separation
 Transport_Aldosterone-mediated regulation of ENaC sodium transport

Elements only in "XPCp0.01" (4 pathways)

Cell cycle_Start of DNA replication in early S phase
 Development_Mu-type opioid receptor signaling via Beta-arrestin
 Nitrogen metabolism/Rodent version
 Glycine, serine, cysteine and threonine metabolism

Common elements in "XPAp0.01" and "XPCp0.01" (2 pathways)

Immune response_Classical complement pathway
 Immune response_Alternative complement pathway

Common elements in "WTp0.01" and "XPCp0.01" (4 pathways)

Cell adhesion_Chemokines and adhesion
 Cell cycle_ESR1 regulation of G1/S transition
 Immune response_IL-15 signaling
 Cell adhesion_ECM remodeling

Elements only in "WTp0.01" (30 pathways)

Development_Glucocorticoid receptor signaling
 Glutathione metabolism / Human version
 Development_EGFR signaling pathway
 Development_IGF-1 receptor signaling
 Immune response_HMGB1/RAGE signaling pathway
 Development_Gastrin in cell growth and proliferation
 n-6 Polyunsaturated fatty acid biosynthesis
 n-3 Polyunsaturated fatty acid biosynthesis
 Mucin expression in CF via TLRs, EGFR signaling pathways
 Transcription_Ligand-dependent activation of the ESR1/SP pathway
 Transport_RAN regulation pathway
 Signal transduction_PKA signaling
 Development_WNT signaling pathway. Part 2
 Immune response_Fc epsilon RI pathway
 PGE2 pathways in cancer
 Transcription_Role of Akt in hypoxia induced HIF1 activation
 Mitochondrial ketone bodies biosynthesis and metabolism
 Immune response_HMGB1 release from the cell
 Transcription_ChREBP regulation pathway
 Development_A3 receptor signaling
 Immune response_CD40 signaling
 Apoptosis and survival_Lymphotoxin-beta receptor signaling
 Transport_Rab-9 regulation pathway
 Development_Angiopoietin - Tie2 signaling
 Apoptosis and survival_HTR1A signaling
 Transcription_Role of heterochromatin protein 1 (HP1) family in transcriptional silencing
 Regulation of metabolism_Role of Adiponectin in regulation of metabolism
 Immune response_IL-1 signaling pathway
 Apoptosis and survival_Beta-2 adrenergic receptor anti-apoptotic action
 Role of prenatal nicotine exposure in apoptosis and proliferation of pancreatic beta cells

Elements only in "XPAp0.01":

Protein folding and maturation_POMC processing
 Apoptosis and survival_TNFR1 signaling pathway
 G-protein signaling_RhoA regulation pathway
 Apoptosis and survival_Role of IAP-proteins in apoptosis
 Development_Inhibition of angiogenesis by PEDF
 Chemotaxis_Lipoxin inhibitory action on fMLP-induced neutrophil chemotaxis
 Development_MAG-dependent inhibition of neurite outgrowth
 Regulation of lipid metabolism_RXR-dependent regulation of lipid metabolism via PPAR, RAR and VDR
 Oxidative stress_Angiotensin II-induced production of ROS
 Regulation of CFTR activity (norm and CF)
 Apoptosis and survival_Caspase cascade
 Blood coagulation_GPCRs in platelet aggregation
 Apoptosis and survival_Role of CDK5 in neuronal death and survival
 Muscle contraction_GPCRs in the regulation of smooth muscle tone
 Cell cycle_Chromosome condensation in prometaphase
 Triacylglycerol metabolism p.1
 Cell cycle_Role of 14-3-3 proteins in cell cycle regulation